4. G.J. Foschini,\Layered space-time architecture for wireless communication in a fading environment when using multi-element antennas, Bell Labs Tech J (1996), 41–59.
5. C.J. Panagamuwa, A. Chauraya, and J.C. Vardaxoglou, Frequency and beam reconfigurable antenna using photoconducting switches, IEEE Trans Antennas Propag 54 (2006), 449–454.
6. Y.K. Park and Y. Sung, A reconfigurable antenna for Quad-band mobile handset applications, IEEE Trans Antennas Propag 60 (2012), 3003–3006.
7. J.H. Lee, Y. Sung, A reconfigurable PIFA using a PIN-diode for LTE/GSM850/GSM900/DCS/PCS/UMTS, Antennas and Propagation Society International Symposium (APSURSI), 2012 IEEE, pp. 1, 2, 8–14 July 2012.
8. C. Aykut, F. Ferrero, L. Cyril, J. Gilles, E. Larique, R. Robin, B. Patrice, Tunable antennas using MEMS switches for LTE mobile terminals, In Proceedings, Loughborough Antennas and Propagation Conference, November, 2013.
9. S.W. Lee, Y. Sung, J.Y. Park, S.J. Lee, and B.J. Hur, Frequency reconfigurable antenna using a PIN diode for mobile handset application, 2013 7th European Conference on Antennas and Propagation (EuCAP), pp. 2053, 2054, 8–12 April 2013.
10. T. Aboufoul, Novel and compact reconfigurable antennas for future wireless configurations, Ph.D. thesis, Department of Electronic Engineering, Queen Mary University of London, United Kingdom, 2014.
11. Y.-L. Ban, Z.X. Chen, Z. Chen, K. Kang, and J.L.W. Li, Reconfigurable narrow-frame antenna for heptaband WWAN/LTE smartphone applications, IEEE Antennas Wireless Propag Lett 13 (2014), 1365–1368.
12. Y. Sung, Multi-band reconfigurable antenna for mobile handset applications, IET Microwaves Antennas Propag 8 (2014), 864–871.
13. Y. Cai, and Z. Du, A novel pattern reconfigurable antenna array for diversity systems, IEEE Antennas Wireless Propag Lett 8 (2009), 1227–1230.
14. Decoupled hepta-band antenna array for WWAN/LTE smartphone applications, IEEE Antennas Wireless Propag Lett 13 (2014), 999–1002.
15. Decoupled planar WWAN antennas with T-shaped protruded ground for smartphone applications, IEEE Antennas Wireless Propag Lett 13 (2014), 483–486.
16. Decoupled closely-spaced hepta-band antenna array for WWAN/LTE smartphone applications, IEEE Antennas Wireless Propag Lett 13 (2014), 31–34.
17. Y.-J. Ren, Ceramic based small LTE MIMO handset antenna, IEEE Trans Antennas Propag 61 (2013), 934–938.
18. K. Kumar Kishor and S.V. Hum, A pattern reconfigurable Chassis-mode MIMO antenna, IEEE Trans Antennas Propag 62 (2014), 3290–3298.
19. C. Rhee, Y. Kim, T. Park, S-s. Kwoun, B. Mun, B. Lee, and C. Jung, Pattern-reconfigurable MIMO antenna for high isolation and low correlation, IEEE Antennas Wireless Propag Lett 13 (2014), 1373–1376.
20. W. Yan and Z. Du, A wideband Quad–antenna system for mobile terminals, IEEE Antennas Wireless Propag Lett 13 (2014), 1521–1524.
21. S. Zhang, K. Zhao, Z. Ying, and S. He, Investigation of diagonal antenna-Chassis mode in mobile terminal LTE MIMO antennas for bandwidth enhancement, IEEE Antennas Propag Mag 57 (2015), 217–228.
22. CST Microwave Studio®, Computer Simulation Technology Homepage. http://www.cst.com.
23. Radio Electronics, Resources and analysis for electronic engineers, LTE frequency bands and spectrum allocations, http://www.radio-electronics.com/info/cellulartelecomms/lte-long-term-evolution/lte-frequency-spectrum.php.
24. C.A. Balanis, Antenna theory analysis and design, 3rd ed., Wiley, New York, ISBN 0-471-66782-X, 2005.
25. D.M. Pozar and B. Kaufman, Comparison of three methods for the measurement of printed antenna efficiency, IEEE Trans Antennas Propag 36 (1988), 136–139.
26. C.C. Chiau, Study of the Diversity Antenna Array for the MIMO Wireless Communication Systems, Ph.D. Thesis, Queen Mary University of London, April 2006.
27. R.G. Vaughan and J.B. Anderson, Antenna diversity in mobile communications, IEEE Trans Veh Technol 36 (1987), 149–172.

A DIFFERENTIAL-FED YAGI–UDA ANTENNA WITH ENHANCED BANDWIDTH VIA ADDITION OF PARASITIC RESONATOR

Yu Luo,[1] Qing-Xin Chu,[2] and Jens Bornemann[1]
[1] Department of Electrical and Computer Engineering, University of Victoria, Victoria, BC V8W 2Y2, Canada; Corresponding author: j.bornemann@ieee.org
[2] School of Electronic and Information Engineering, South China University of Technology, Guangzhou, Guangdong 510640, China

Received 6 June 2016

ABSTRACT: *A printed-circuit differential-fed Yagi–Uda antenna is presented that features enhanced bandwidth by employing a parasitic quarter-wavelength coplanar stripline (CPS) resonator which adds one more resonant mode within the operating bandwidth. The proposed antenna is designed, fabricated and measured. Experimental results are in good agreement with simulations. In the band of 2.27–2.58 GHz, the return loss is better than 10 dB and the gain better than 6 dBi.* © 2016 Wiley Periodicals, Inc. Microwave Opt Technol Lett 59:156–159, 2017; View this article online at wileyonlinelibrary.com. DOI 10.1002/mop.30253

Key words: *Yagi–Uda antenna; parasitic resonator; enhanced bandwidth*

1. INTRODUCTION

Increasing requirements in the wireless communication market demand integrated and compact radio frequency (RF) front-end products which are fully compatible with differential signal operation [1,2]. Due to their excellent potential in terms of radiation pattern and frequency agility, parasitic element antennas (PEAs) are widely implemented in modern communication systems [3,4]. Compared with a single antenna element, the PEA provides a larger degree of freedom and eliminates bulky feed distribution networks of antenna arrays. As a typical kind of PEA, Yagi–Uda antennas are widely employed in modern communication systems [5–12]. However, many Yagi–Uda antenna designs are single-ended and thus incompatible with fully integrated RF front-end products.

In this paper, a new printed-circuit differential-fed Yagi–Uda antenna is presented that achieves enhanced bandwidth by employing a parasitic coplanar stripline (CPS) resonator. The advantage of this design is threefold: first, it increases the bandwidth while maintaining a gain better than 6 dBi; secondly, it improves the return loss; and thirdly, it provides a differential feed as required in modern RF front ends. The antenna is designed, fabricated and measured, and experiments validate the design approach.

2. ANTENNA DESIGN AND CHARACTERISTICS

The layout of the proposed printed-circuit differential-fed Yagi–Uda antenna is shown in Figure 1; its dimensions are summarized in Table 1. The proposed antenna is printed on a substrate

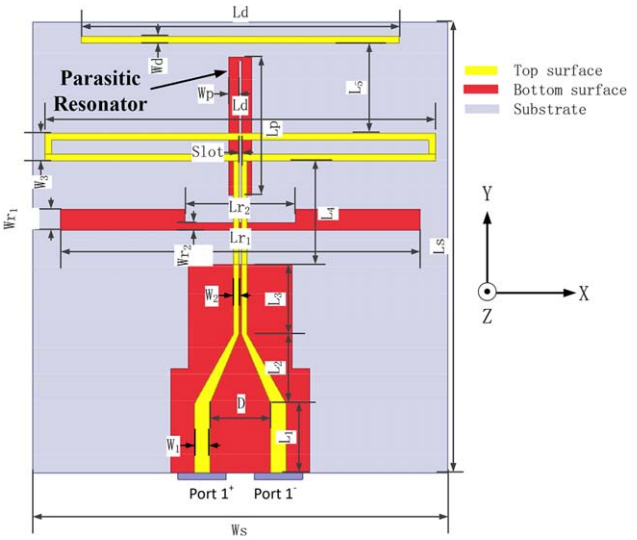

Figure 1 Layout of the proposed antenna. [Color figure can be viewed at wileyonlinelibrary.com]

TABLE 1 Dimensions of the Proposed Antenna

Parameter	W_s	L_s	L_1	L_2	L_3	L_4	L_5	P_p
Value (mm)	60	65	10	10	10	15	13	40
Parameter	D	W_{r1}	W_{r2}	L_{r1}	L_{r2}	W_3	L_d	
Value (mm)	8.8	3	1	52	16	4	56.4	
Parameter	W_1	W_2	Slot	W_d	W_p	L_p	L_d	
Value (mm)	2.2	1	0.4	1	1.5	20	56	

with thickness of 0.8 mm and relative permittivity of $\varepsilon_r = 2.55$. The parasitic CPS resonator is shown on the bottom surface. As usual, the Yagi–Uda antenna comprises a folded dipole, a director and a reflector. To reduce the footprint of this antenna, a stepped-width reflector is employed as previously investigated in [12].

Figure 2 shows the effect of the parasitic resonator on the differential reflection coefficient $|S_{diff11}|$. The bandwidth enhancement is clearly demonstrated when using the parasitic quarter wavelength CPS resonator depicted in Figure 1.

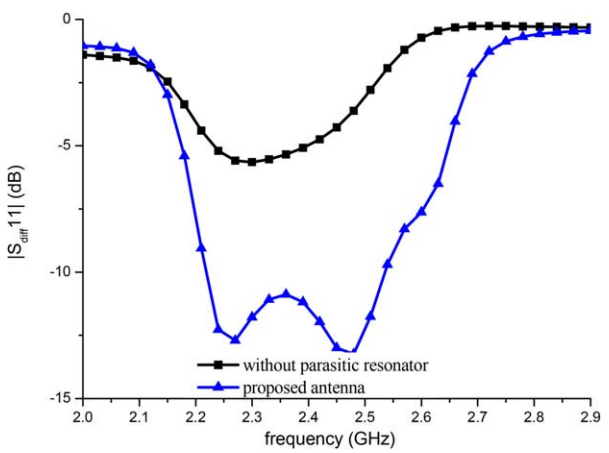

Figure 2 Effects of parasitic elements on $|S_{diff11}|$. [Color figure can be viewed at wileyonlinelibrary.com]

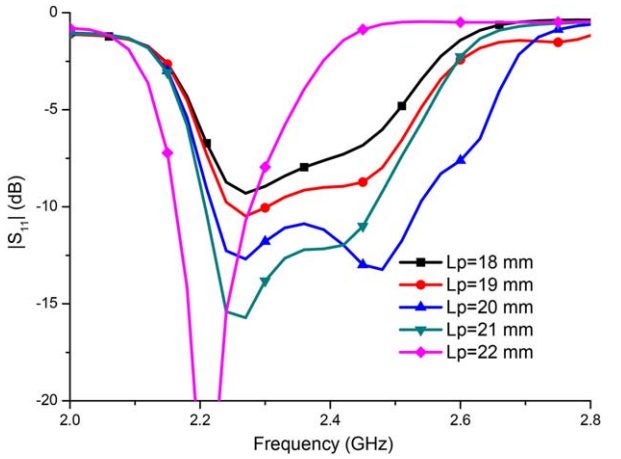

Figure 3 Effects of L_p on $|S_{diff11}|$. [Color figure can be viewed at wileyonlinelibrary.com]

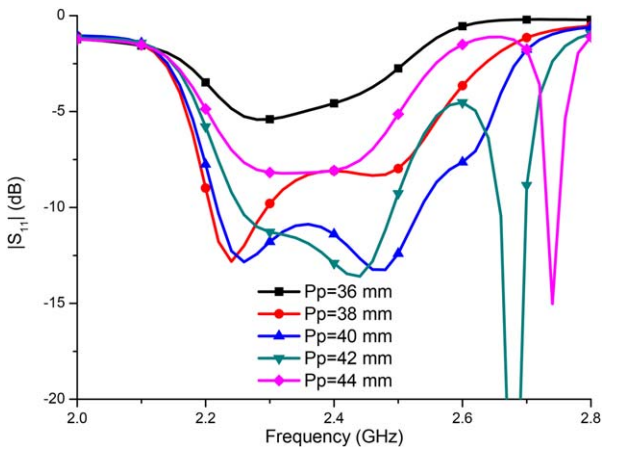

Figure 4 Effects of P_p on $|S_{diff11}|$. [Color figure can be viewed at wileyonlinelibrary.com]

Without this resonator, only a single resonance is in effect, providing a minimum reflection coefficient of only −5 dB. After the addition of the parasitic resonator, we observe two

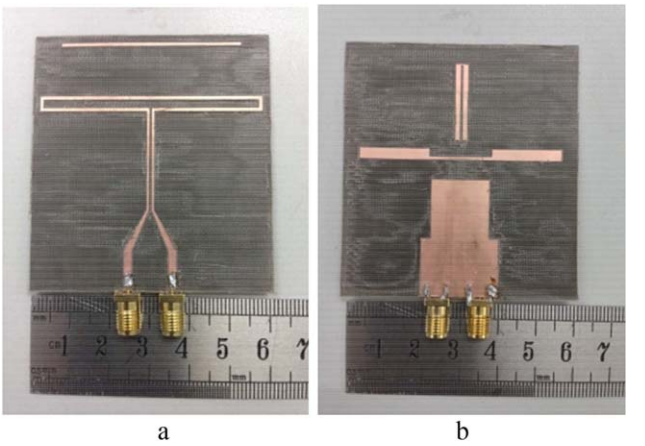

Figure 5 Top- and bottom view photographs of the fabricated antenna: a top view, b bottom view. [Color figure can be viewed at wileyonlinelibrary.com]

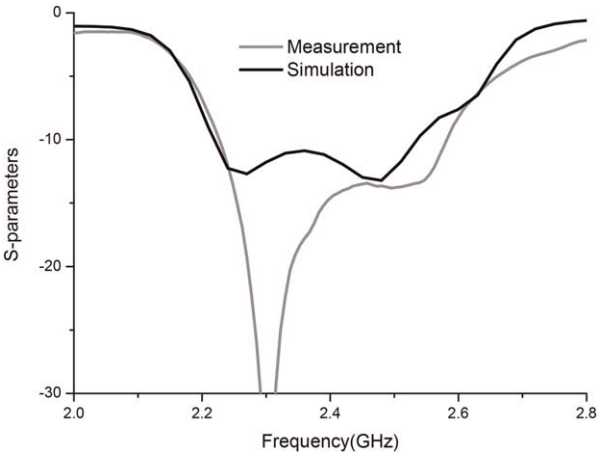

Figure 6 Simulated and measured $|S_{diff11}|$

resonances, and the reflection coefficient improves to better than −10 dB over a 10 dB return-loss frequency band of 2.23–2.55 GHz.

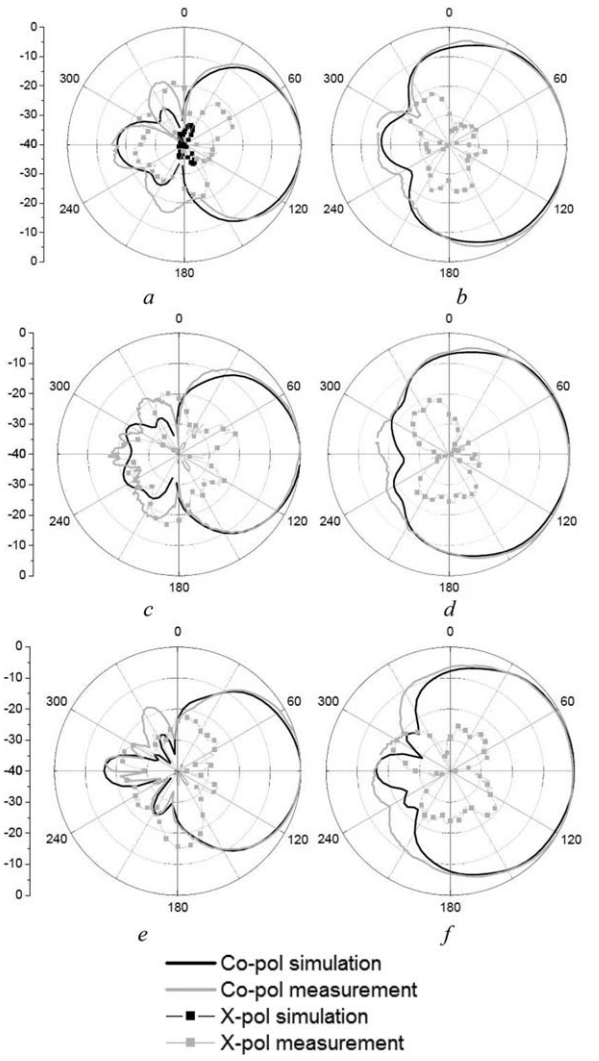

Figure 7 Simulated and measured normalized radiation patterns. a 2.3 GHz *xy* plane, b 2.3 GHz *yz* plane, c 2.4 GHz *xy* plane, d 2.4 GHz *yz* plane, e 2.5 GHz *xy* plane, f 2.5 GHz *yz* plane

TABLE 2 Gains of the Proposed Antenna

Frequency	2.3 GHz	2.4 GHz	2.5 GHz
Simulated gain (dBi)	6.9	6.9	7.2
Measured gain (dBi)	6.1	6.5	6.2

To understand how the parasitic resonator affects $|S_{diff11}|$, the lengths of the parasitic resonator (L_p) and their positions (P_p) are studied.

The effects of L_p on $|S_{diff11}|$ are shown in Figure 3. When L_p = 18 mm, $|S_{diff11}|$ fails to reach −10 dB in the desired band. When L_p increases, $|S_{diff11}|$ improves and settles at values below −10 dB in the band of 2.23–2.55 GHz. Beyond L_p = 20 mm, the bandwidth narrows again.

Figure 4 exhibits the effect of the position P_p of the parasitic resonator on $|S_{diff11}|$. With P_p = 36 mm, $|S_{diff11}| < -10$ dB cannot be obtained in the desired band. As P_p increases, $|S_{diff11}|$ improves and achieves values below −10 dB in the band of 2.23–2.55 GHz for P_p = 40 mm. Beyond P_p = 40 mm, the bandwidth decreases and reflection coefficient $|S_{diff11}|$ increases.

To verify the design procedure, a prototype is fabricated as shown in Figure 5. Measurements on differential input reflection coefficient, gain and radiation patterns are performed using an Agilent E5071B vector network analyzer and a far-field antenna testing system with a 180° hybrid coupler as introduced in [13]. Figure 6 depicts a comparison between simulation and measurement of the reflection coefficient. Good agreement between experiment and simulation is observed. The measured results demonstrate that the reflection coefficient is below −10 dB in the band of 2.27–2.58 GHz. The lower resonance is more pronounced in the measurements than the second one. We attribute this fact to manufacturing tolerances.

Simulated and measured radiation patterns in both *xy*- and *yz* planes (c.f. Fig. 1) are shown in Figure 7 for three different frequencies. Directive patterns with 17 dB front-to-back ratio are obtained, and the crosspolarization level is down by more than 20 dB.

Gain measurements at 2.3, 2.4, and 2.5 GHz are presented in Table 2. The measured gain is better than 6 dBi, however, it is up to 1 dB below the simulations. We attribute this fact to the loss of the 180° coupler [13] which is included in the measurements to differentially feed the antenna.

3. CONCLUSION

A differential-fed Yagi–Uda antenna with enhanced bandwidth is proposed, designed and experimentally verified. Bandwidth enhancement is achieved by a parasitic resonator that provides an additional resonating mode. In the band of 2.27–2.58 GHz, about 6 dBi gain, 10 dB return loss and 17 dB front-to-back ratio are achieved by the antenna. Measured results verify the design procedure.

ACKNOWLEDGMENTS

This work was supported in part by the by the National Natural Science Foundation of China (61171029).

REFERENCES

1. C.H. Wang, Y.H. Cho, C.S. Lin, H. Wang, C.H. Chen, D.C. Niu, J. Yeh, C.Y. Lee, and J. Chem, A 60 GHz transmitter with integrated antenna in 0.18 m SiGe BiCMOS technology, IEEE Int Solid-State Circuit Conf Tech Dig (2006), San Fransisco, CA, 186–187.
2. C.H. Wu, C.H. Wang, and C.H. Chen, Balanced coupled-resonator bandpass filters using multisection resonators for common-mode

suppression and stopband extension, IEEE Trans Microw Theory Tech 55 (2007), 1756–1763.
3. C.J. Panagamuwa, A. Chauraya, and J.C. Vardaxoglou, Frequency and beam reconfigurable antenna using photoconducting switches, IEEE Trans Antennas Propag 54 (2006), 449–454.
4. F. Fezai, C. Menudier, and M. Thévenot, Systematic design of parasitic element antennas—Application to a WLAN Yagi design, IEEE Antennas Wireless Propag Lett 12 (2013), 413–416.
5. H. Yagi, Beam transmission of ultra short waves, Proc Inst Radio Eng 16 (1928), 715–740.
6. D.M. Pozar, Beam transmission of ultra short waves: an introduction to the classic paper by H. Yagi, Proc IEEE 85 (1997), 1857–1863.
7. P.R. Grajek, B. Schoenlinner, and G.M. Rebeiz, A 24-GHz high-gain Yagi–Uda antenna array, IEEE Trans Antennas Propag 52 (2004), 1257–1261.
8. A.C.K. Mak, C.R. Rowell, and R.D. Murch, Low cost reconfigurable Landstorfer planar antenna array, IEEE Trans Antennas Propag 57 (2009), 3051–3061.
9. K. Han, Y. Park, and H. Choo, Broadband CPS-fed Yagi–Uda antenna, IET Electron Lett 45 (2009), 1207–1208.
10. A.D. Capobianco, F.M. Pigozzo, and A. Assalini, A compact MIMO array of planar end-fire antennas for WLAN applications, IEEE Trans Antennas Propag 59 (2011), 3462–3465.
11. J. Wu, Z. Zhao, and Z. Nie, A broadband unidirectional antenna based on closely spaced loading method, IEEE Trans Antennas Propag 61 (2013), 109–116.
12. Y. Luo and Q.X. Chu, A Yagi–Uda antenna with a stepped-width reflector shorter than the driven element, IEEE Antennas Wireless Propag Lett 15 (2016), 564–567.
13. Y. Luo and Q.X. Chu, Oriental crown-shaped differentially fed dual-polarized multi-dipole antenna, IEEE Trans Antennas Propag 63 (2015), 4678–4685.

LOG PERIODIC SLOT-LOADED CIRCULAR VIVALDI ANTENNA FOR 5–40 GHZ UWB APPLICATIONS

Waqas Mazhar, David Klymyshyn, and Aqeel Qureshi
Department of Electrical and Computer Engineering,
University of Saskatchewan, Saskatoon, SK,
Canada; Corresponding author: waqas.mazhar@usask.ca

Received 6 June 2016

ABSTRACT: *A compact antipodal log periodic slot-loaded circular Vivaldi antenna with dimension (*L × W*) 45 × 60mm is presented. Structural modification to the conventional antipodal Vivaldi antenna results in miniaturization, improved impedance and pattern bandwidth performance. Proposed designs are prototyped and measured to validate wide-impedance bandwidths from 5 to 40 GHz. These are compared to measurements on similarly fabricated traditional antipodal and circular Vivaldi antennas which shows a bandwidth only up to 26 GHz. In addition, the measured antenna gain and radiation efficiency of the log periodic slot-loaded circular Vivaldi antenna are also found higher than the conventional designs.* © 2016 Wiley Periodicals, Inc. Microwave Opt Technol Lett 59:159–163, 2017; View this article online at wileyonlinelibrary.com. DOI 10.1002/mop.30252

Key words: *antipodal; slot; log periodic; impedance bandwidth; efficiency; fabricated; Vivaldi antenna*

1. INTRODUCTION

Recently, much progress has been made in ultra-wideband (UWB) applications focused on high data rates and low fabrication cost. As an integral component of these UWB systems, antennas face serious challenges to achieve compact size, wide-impedance bandwidth, linear group delay, and stable radiation patterns [1].

The Vivaldi antenna was first analyzed by Gibson in 1971. Since then it has been extensively studied and used due to its low cost, light weight, wide-impedance bandwidth, and high gain features. It has been widely utilized, for instance, in ground penetrating radars. Theoretical analysis of Vivaldi antennas is discussed in Refs. 2,3. The Vivaldi antenna takes advantage of both coplanar and antipodal geometry. The coplanar Vivaldi antennas [4] are typically limited by their feed transitions, i.e., microstrip to slotline, which results in both high radiation loss and distorted radiation patterns at high frequencies. The Antipodal Vivaldi antennas also suffer from high cross polarization [5] although they usually have higher bandwidth, i.e., >10:1, in comparison to coplanar Vivaldi antennas.

The antenna size is also critical for many applications like aircraft, armored vehicles, tactical radios, and many other compact handheld devices. Reducing the antenna size not only limits its bandwidth but also results in degradation of gain and efficiency. Therefore various techniques have been developed to improve the performance of the miniaturized antennas for different applications. Considerable research has been conducted to improve the efficiency of Vivaldi antennas however few articles address the antenna miniaturization [9–11]. According to literature, the minimum size of the Vivaldi antenna is about $0.5\lambda_0$, although they typically require a much larger antenna size to attain good performance. In Refs. [6,7], tapering of the edges is done to improve the impedance bandwidth and radiation pattern. A compact antipodal Vivaldi antenna is presented in Ref. [8], which has relatively low gain. A step connection structure is proposed in Ref. [12] providing a gain of up to 6 dBi. Elliptical tapering is demonstrated in Ref. [13] to provide a large impedance bandwidth of 9 GHz. In Ref. [11], it was shown that slot-loading of the circular-type flares could increase the directivity providing increased gain, particularly in the higher frequency portion of the band.

In this article, a Vivaldi antenna with slot-loaded circular flares is presented. In this case, the slots are arranged in a log periodic fashion, to simultaneously provide broad impedance bandwidth, and significantly increased gain in the upper region of the band. To validate the significance of this approach, a conventional antipodal Vivaldi antenna and a Vivaldi antenna with simple non-slotted circular flares are prototyped and measured. The results show that the addition of the log periodic slots in the circular Vivaldi antenna enhances its directivity and bandwidth at higher frequencies as compared to the conventional designs. The antenna structures along with the feeding mechanism shown in Figure 1 have a simulated and measured peak gain of 12 dBi over a bandwidth of 5 to 40 GHz. The simulated and measured group delay is also provided for visualizing the frequency dispersion across the operational bandwidth. The addition of log periodic slots in circular Vivaldi antennas has a performance improvement over other compact Vivaldi antennas [8–10], and also a size miniaturization as compared to previous designs [10,14].

2. PROPOSED ANTENNA DESIGN

The geometry of the designed antennas is presented in Figure 1 which demonstrates the progression from conventional Vivaldi antenna toward the log periodic slot-loaded Vivaldi antenna. Figure 1(a) presents a simple antipodal Vivaldi antenna. In Figure 1(b) the antipodal Vivaldi antenna flares are terminated with